

TARGETING MAGNETIC CARRIER PARTICLES IN TUMOUR MICROVASCULATURE – A NUMERICAL STUDY

O. Rotariu^{a,b*}, L. E. Udrea^a, N. J. C. Strachan^b, V. Bădescu^a

^aNational Institute of Research and Development for Technical Physics –I.F.T., Iasi, 700050, Romania

^bUniversity of Aberdeen, School of Biological Sciences, Aberdeen, AB24 3UU, United Kingdom

The delivery of anticancer agents via magnetic carrier particles is an exciting new prospect in treating cancer. The targeting of tumours situated at large distances from the surface of the human body is difficult because the magnetic force decreases rapidly with the distance from the magnets. Here numerical modelling is used to investigate physical and physiological limits that influence the focus of small magnetic particles (MPs) within the microvasculature of tumours. Methods using systems of permanent magnets were found to have a range of capture < 12 centimetres and this depends on the blood flow rate, the magnetic field, the MPs properties, the length of blood vessels and their diameters. These results indicate that this methodology is suitable for treating sub-surface cancers within the human body.

(Received July 19, 2005; accepted November 24, 2005)

Keywords: Magnetic drug targeting, Magnetic particles, Blood flow, Capillaries, Arterioles and small arteries, Mathematical modelling.

1. Introduction

Magnetic drug delivery (MDD) is a new technique for targeted and controlled release of anticancer agents inside the human body. Its feasibility has been proven for surface tumours on small animals and in clinical tests on 14 patients [1 - 3]. However, despite the real progress achieved with these trials, a series of technical and physiological problems hinder the application of the method in the clinical practice.

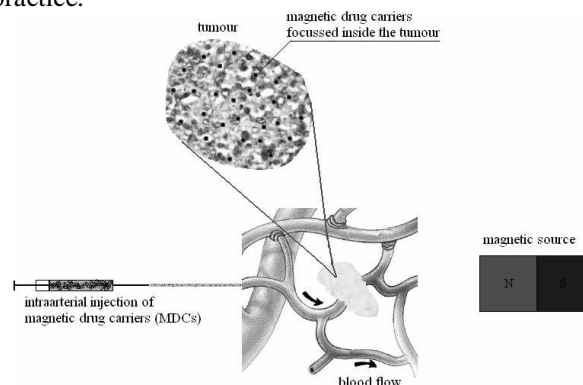


Fig.1. Schematic diagram of the magnetic drug delivery method. The Magnetic Drug carriers (MDCs) loaded with an anticancer drug are injected within a main artery in the proximity of the tumour. The sanguine flux transports the MDCs to the tumour, which are retained there under the influence of the external magnetic field.

* Corresponding author: leus@phys-iasi.ro

The principle of MDD method is simple and consists in the injection of magnetic drug carriers (MDCs) within the blood stream, followed by their retention at the target site, under the presence of an external gradient magnetic field (Figure 1). The MDCs retained inside the small blood vessels or within the tumoural tissues, slowly release the chemotherapeutic drug and inducing necrosis of the cancer cells. The main advantage of this technique is the treatment of the cancer whilst causing minimal affects on the surrounding healthy tissues.

A specification of what is needed for the intratumoural MDT was made elsewhere [4, 5]. A major problem is that of targeting areas positioned deep inside the human body. This paper presents a numerical study of the non-invasive capture of the MDCs within the microvasculature of diseased and normal blood vessels, which are positioned at various distances within the human body. The maximum distance (x_{\max}) from the magnetic source for the efficient capture of MDCs is computed. This is achieved by modelling the particle trajectories and stochastic simulation for various flow velocities, blood vessel geometry, magnetic field strengths and particle properties.

2. Numerical models

2.1. Forces in MDCs targeting

Basically, the motion of MDCs within the blood vessels when subjected to an external magnetic field is affected by the magnetic force and the hydrodynamic drag force. Depending on the relative orientation of magnetic and drag forces, there are three geometrical configurations of interest (Figure 2): (i) the flow points towards the magnetic source; (ii) the flow is perpendicular to the magnetic force (iii) the flow points in the opposite direction to the magnetic source. If the volume concentration of MDCs is $>1\%$ then their magnetic dipolar interactions may lead to aggregation of particles. Moreover, the aggregation process is strongly influenced by the magnetostatic interaction between the MDCs and the magnetic field.

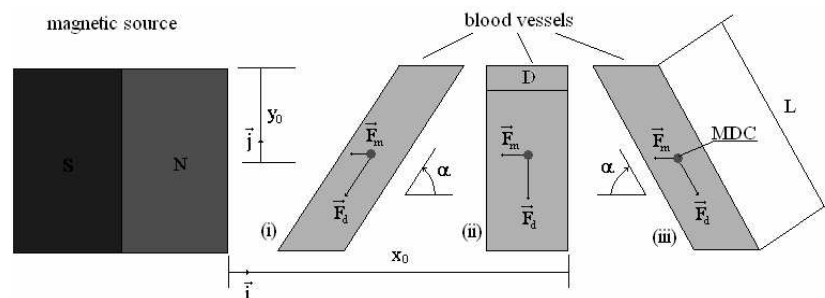


Fig. 2 .Geometrical configurations of interest in MDCs targeting for three blood vessels pointing: (i) towards the magnetic source; (ii) perpendicular to the magnetic force; (iii) in the opposite direction to the magnetic force. L , D , and α are the length, the diameter and the orientation of the blood vessels against the magnetic force. x_0 and y_0 are the initial coordinates of MDCs.

The magnetic force acting on MDCs is [6]

$$\vec{F}_M = \mu_0 V_p M_p \nabla H, \quad (1)$$

where $\mu_0 (= 4\pi \times 10^{-7} \text{ H/m})$ is the magnetic permeability of the void space, $V_p = \frac{\pi d^3}{6}$ is the volume of MDCs of diameter d , M_p their magnetization and H the intensity of the magnetic field.

The hydrodynamic drag force acting on MPs can then be given by Stokes formula [7]

$$\vec{F}_D = -3\pi\eta d(\vec{v}_p - \vec{v}_0) \quad (2)$$

where $\vec{v}_p = \frac{dx}{dt} \vec{i} + \frac{dy}{dt} \vec{j}$ is the velocity of MDCs in a 2D system with \vec{i} and \vec{j} being unit vectors, \vec{v}_0 is the velocity of blood and η its dynamic viscosity coefficient.

The magnetic dipolar energy between MDCs is

$$U_{dip} = \frac{\mu_0 m^2}{4\pi d^3} \sum_{i \neq j} \frac{1 - 3 \cos^2(\vec{r}_{ij}, \vec{m})}{r_{ij}^3 / d^3} \quad (3)$$

\vec{m} being the dipolar magnetic moment of the MDCs and r_{ij} their relative position.

The orientation of the MDCs dipolar magnetic moments is characterized by the magnetostatic interaction energy

$$U_H = -\mu_0 \vec{m} \cdot \vec{H}. \quad (4)$$

Taking into account the above two energies and the Brownian motion, the behaviour of a system of magnetic particles subjected to an external magnetic field can be characterized by two constants, $\lambda = \mu_0 m^2 / 4\pi d^3 kT$ and $\xi = \mu_0 mH / kT$, which compares the strength of the magnetic dipolar and magnetostatic interactions with the thermal energy kT (T being the temperature and $k = 1.38 \cdot 10^{-23} \text{ J/K}$ the Boltzmann constant) [8].

2.2. Magnetic field configuration

The non-invasive MDT uses permanent magnets or electromagnets positioned outside the human body in the proximity of the tumours. For this study an array of rectangular magnets ($50 \times 50 \times 12.5 \text{ mm}$) (Sintered NdFeB, 35 MGOe, 50x50x12.5 mm, MMG MagDev Ltd., Swindon, UK) have been simulated using the 2D “Finite Element Method Magnetics” program (FEMM3.2) from Foster-Miller (<http://femm.foster-miller.com>). The magnetic field structure (flux lines and qualitative density plot of the induction of the magnetic field) is presented in Figure 3 for 5 magnets.

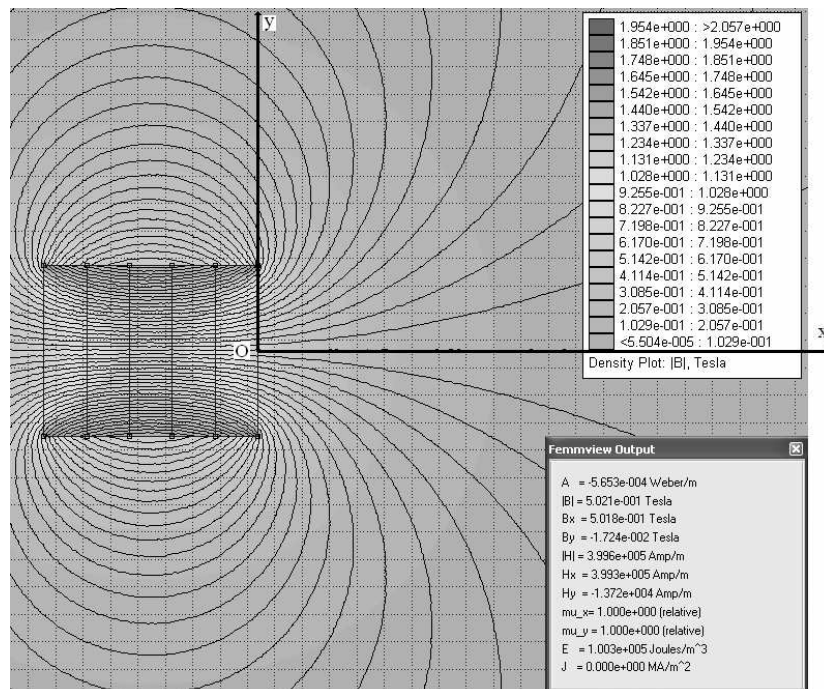


Fig. 3. 2D map of the magnetic field for an array of 5 rectangular magnets.

The active component of the magnetic field, which pulls the MDCs from the sanguine flux is the horizontal one, H_x . The numerical data for H_x , measured on the symmetry axis of the magnetic system ($y = 0$), is fitted with an exponential function,

$$H_x(y = 0) = H_0 \exp(-x/a), \quad (5)$$

where H_0 is the intensity of the magnetic field on the surface of the magnetic system and a a fitting factor having the dimension of length. The fitting data corresponding to figure 3 give $H_0 \approx 500 \text{ kA/m}$ and $a = 2.5 \text{ cm}$. However, in the following simulations the intensity of the magnetic field will vary in the range $H_0 \in [100, 500] \text{ kA/m}$.

2.3 .Particle aggregation and the equations of particle trajectories

A Metropolis Monte Carlo model [9, 10] is used to simulate the aggregation between MDCs subjected to the action of the horizontal magnetic field. Basically, the protocol presented in [9] consists in the minimization of the energy (eqs. 3 and 4) for a system of N particles. In the simulations particles with strong dipolar interactions have the potential of aggregating, at particle volume/surface concentrations ~ 0.01 , which is smaller than that required to cause embolization [11]. After aggregation the MDCs move within the blood vessels on trajectories given by

$$\vec{F}_m + \vec{F}_d = \vec{F}_{inertial} \quad (6)$$

where the inertial forces can be neglected for small (micrometer size) particles.

For the three geometrical configurations presented in Figure 2 the equations of the MDCs trajectories are obtained from eqs. (1), (2), (5) and (6) and are

- (i) the blood vessel pointing towards the magnetic source
- (ii)

$$y = y_0 + \tan(\alpha)a \text{Log}_e \left[\frac{1 + (v_0/v_m)\cos(\alpha)\exp(x/a)}{1 + (v_0/v_m)\cos(\alpha)\exp(x_0/a)} \right] \quad (7)$$

- (iii) the blood vessel aligned perpendicular to the magnetic force
- (iv)

$$y = y_0 + (v_0/v_m)a(\exp(x/a) - \exp(-x_0/a)) \quad (8)$$

- (iii) the blood vessels pointing in the opposite direction to the magnetic force

$$y = y_0 + \tan(\alpha)a \text{Log}_e \left[\frac{-1 + (v_0/v_m)\cos(\alpha)\exp(x/a)}{-1 + (v_0/v_m)\cos(\alpha)\exp(x_0/a)} \right] \quad (9)$$

where (x_0, y_0) are the initial coordinates of MDCs and α is the angle of the blood vessel orientation to the magnetic force. The MDCs motion is strongly influenced by the system parameters, which are enclosed in so called “magnetic velocity”, $v_m = \mu_0 d^2 H_0 \epsilon M_p / 18 \eta a$ - the terminal velocity of the particle under the influence of the magnetic and drag forces [12].

3. Results and discussion

The aggregation of MDCs is strongly influenced by the magnetic dipolar interactions between particles, the magnetostatic interaction of the particle-magnetic field, and their volume fraction ϕ . Figs. 4 and 5 present aggregates of MDCs and their cluster size distribution for strong magnetic dipolar and magnetostatic interactions ($\lambda = \beta \rightarrow \infty$). The volume fraction of MDCs was

set at a moderate value ($\phi = 0.01$). Basically, clusters with an average size of 3.7 particles/cluster (standard deviation – 2.72) are characteristic for this particle concentration. By the increase of the volume fraction of MDCs, larger clusters and particle structures will appear, which can block both diseased and healthy blood vessels. Therefore, the first condition to obtain selective MDCs capture is to use a small concentration of carrier particles ($\phi < 0.01$).

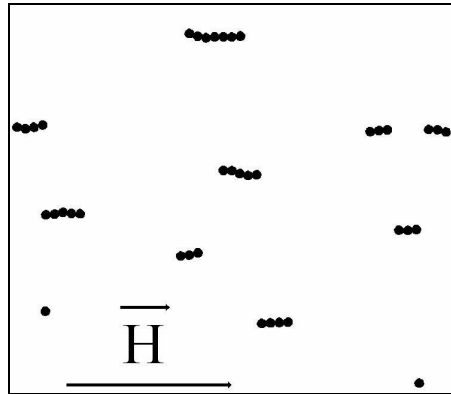


Fig. 4. Aggregates of MDCs subjected to a horizontal magnetic field.

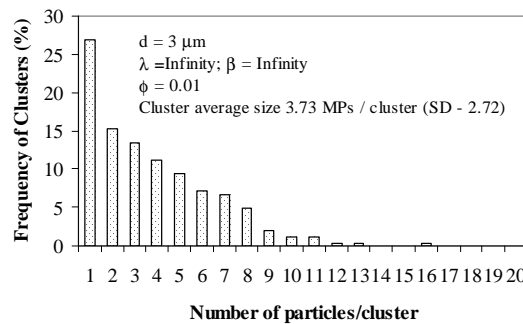


Fig. 5. Cluster size distribution for MDCs aggregates having strong dipolar and magnetostatic interactions ($\lambda = \beta \rightarrow \infty$), and moderate concentration $\phi = 0.01$.

The second condition required for the capture of particles is their deviation from the blood stream and attaching to the blood vessels wall. The factors that influence the particles’ trajectories and the maximum distance (x_{max}) (measured from the surface of the magnetic system) to which the MDCs are captured with high efficiency (100 %) are analysed below.

Figure 6 shows the trajectories of MDCs obtained by solving eq. (8) in *Mathematica 5.0* within two small arteries. The particles are released at the upper part of the blood vessels and are considered captured when they touch the blood vessel’s wall nearest to the magnetic source (left side). If the particles have trajectories (the vertical projection) longer than the length of the blood vessels, they are not captured and hence the recovery is $< 100\%$. The two sets of trajectories differ by the positions of the arteries with respect to the surface of the magnetic system: $x_a = 0.23$ cm in Figure 6 a, and $x_a = 2.63$ cm in Figure 6 b. It is clear that using magnetic systems supplying large magnetic field strengths ($H_0 = 500$ kA/m), it is possible to capture all the magnetite particles ($M_p = 450$ kA/m) of micrometer size ($d = 3.0 \mu m$) and low concentrations ($\phi < 0.01$), within the small arteries positioned close to the magnetic system (Figure 6.a). However, for small arteries situated at medium and large distances ($x_a > 2.5$ cm), the majority of MDCs escape and pass through towards the arterioles and capillaries.

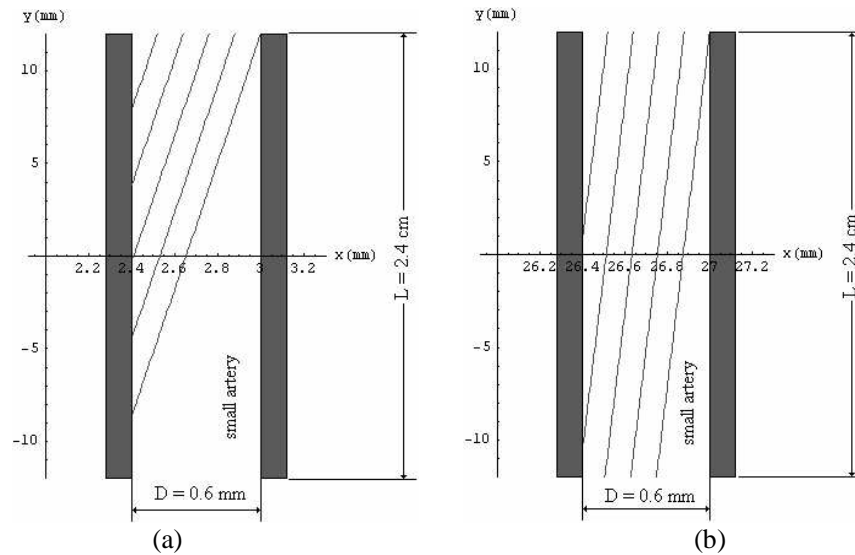


Fig. 6. Trajectories of MDCs in two small arteries: (a) the position of the artery is $x_a = 2.3$ mm and the initial coordinates of the MDCs are $x_0 = (3.0, 2.88, 2.76, 2.64, 2.52)$ mm; (b) the position of the artery $x = 26.3$ mm and the initial coordinates of the MDCs are $x_0 = (27.00, 26.88, 26.76, 26.64, 26.52)$ mm). The remaining parameters are: $y_0 = 12.0$ mm, $d = 3.0$ μm , $M_p = 450$ kA/m (saturation value), $H_0 = 500$ kA/m, $a = 2.5$ cm, $v_0 = 6.0$ cm/s, $\eta = 0.0028$ kg/ms, $D = 0.6$ mm, $L = 2.4$ cm, $\alpha = 90^\circ$ and $\phi < 0.01$.

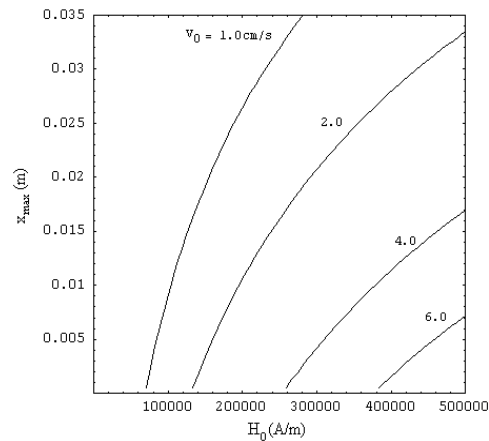


Fig. 7. The maximum capture distance (x_{\max}) of MDCs, for small arteries as a function of the magnetic field strength and blood velocity. The parameters used in the simulation are the same as described for Fig. 6.

The maximum capture distance (x_{\max}) is calculated as a function of the magnetic field strength at the surface of the magnetic system, H_0 , and the results are presented in Figure 7 for a family of four small arteries, which have various blood velocities. It appears that the distance of capture increases when the magnetic field increases and goes up to few centimetres for small blood velocities ($v_0 = 1$ to 2.0 cm/s). However, for larger blood velocities ($v_0 = 6.0$ cm/s) x_{\max} decreases up to a few mm. This means that the MDCs will be retained just at the surface of the human body. This result suggests that a magnetic system based on arrays of permanent magnets can be used for the targeted retention of MDCs just within very small blood vessels (arterioles and capillaries), where the penetration of drugs within the tissue can take place. Therefore, the remainder of this paper concentrates on the analysis of capture of MDCs within arterioles and capillaries.

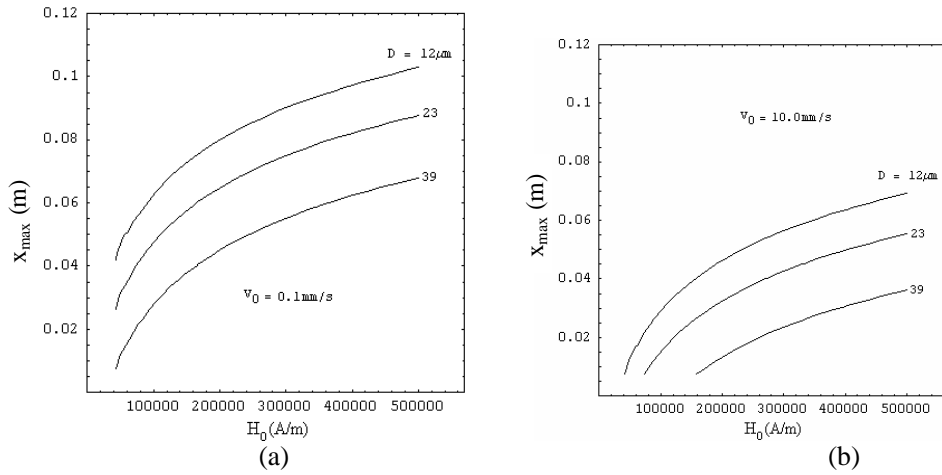


Fig. 8. The maximum capture distance (x_{\max}) of MDCs for arterioles and capillaries vs. the magnetic field strength and blood velocity: (a) $v_0 = 0.1 \text{ mm/s}$; (b) $v_0 = 10.0 \text{ mm/s}$. The diameter of blood vessels is a variable parameter. The remaining parameters are: $y_0 = 0.5 \text{ mm}$, $\eta = 0.0028 \text{ kg/ms}$, $d = 3.0 \mu\text{m}$, $M_p = 450 \text{ kA/m}$, $a = 2.5 \text{ cm}$, $L = 1.0 \text{ mm}$, $\alpha = 90^\circ$ and $\phi < 0.01$.

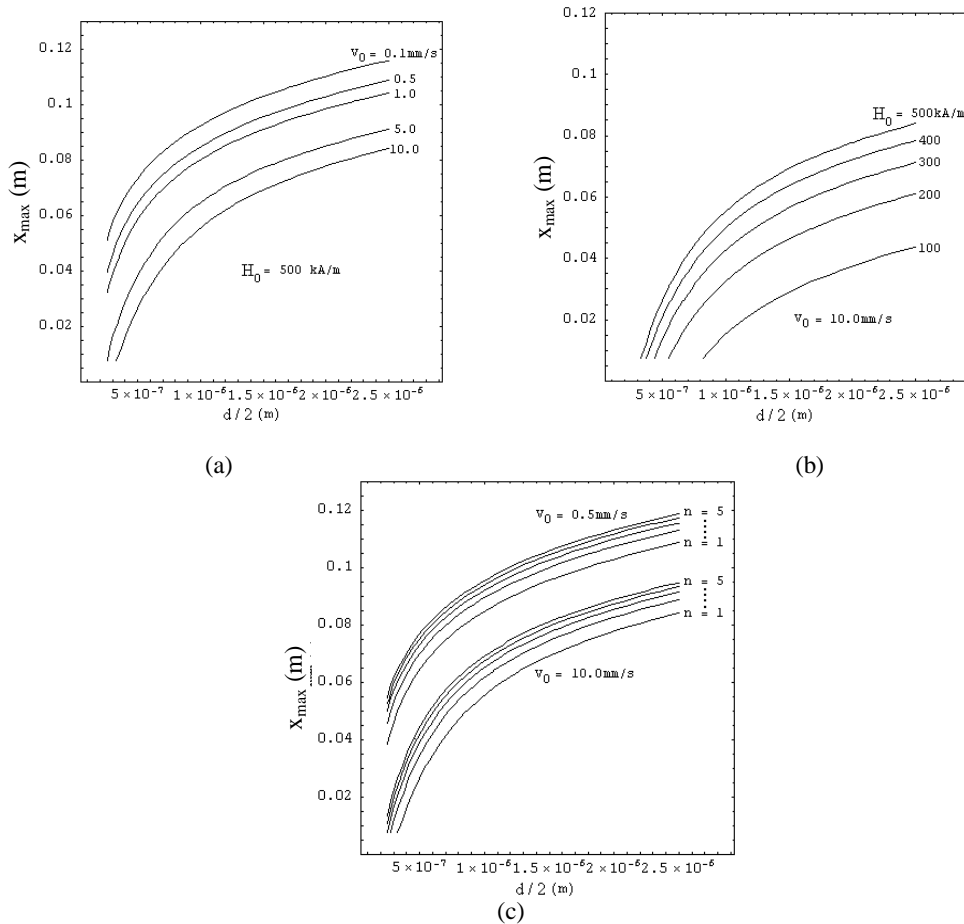


Fig. 9. The maximum capture distance (x_{\max}) of MDCs for arterioles and capillaries as a function of the MDCs diameter: (a) v_0 varies from 0.1 to 10.0 mm/s and $H_0 = 500 \text{ kA/m}$; (b) H_0 varies from 100 to 500 kA/m and $v_0 = 10.0 \text{ mm/s}$; (c) $H_0 = 500 \text{ kA/m}$ and the MDCs are form clusters of size up to $n = 5$ particles. The remaining parameters are: $y_0 = 0.5 \text{ mm}$, $\eta = 0.0028 \text{ kg/ms}$, $M_p = 450 \text{ kA/m}$, $a = 2.5 \text{ cm}$, $D = 12.0 \mu\text{m}$, $L = 1.0 \text{ mm}$, $\alpha = 90^\circ$ and $\phi < 0.01$.

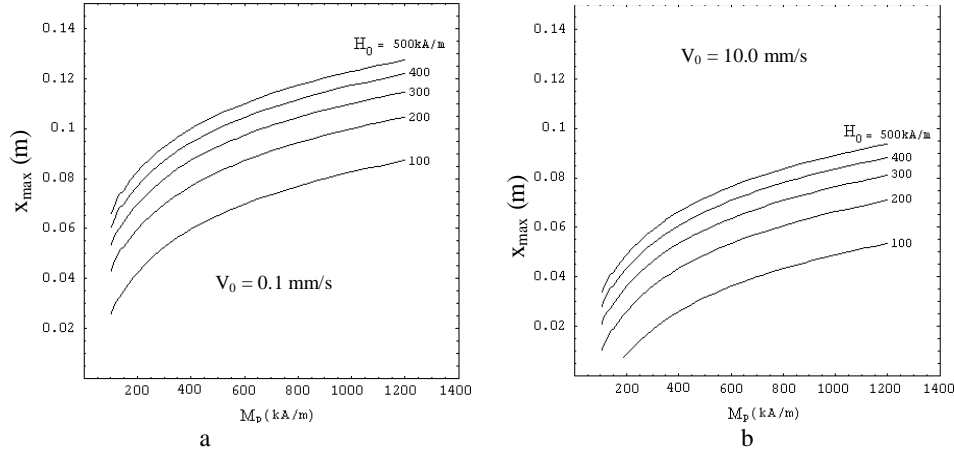


Fig. 10. The maximum capture distance (x_{\max}) of MDCs for arterioles and capillaries as a function of the magnetization of the particles: (a) $v_0 = 0.1$ mm/s; (b) $v_0 = 10.0$ mm/s. The magnetic field strength is a variable parameter. The remaining parameters are: $y_0 = 0.5$ mm, $\eta = 0.0028$ kg/ms, $d = 3.0$ μm , $a = 2.5$ cm, $D = 12.0$ μm , $L = 1.0$ mm, $\alpha = 90^\circ$ and $\phi < 0.01$.

Figs. 8 to 12 present the maximum capture distance (x_{\max}) of MDCs within arterioles and capillaries for various physiological (v_0 , η , D , L , α) and system parameters (H_0 , d , M_p , ϕ , number of particles/ aggregate - n). The characterisation of MDCs capture, within small blood vessels, which are perpendicularly oriented to the magnetic force, is given in Figures 8 to 10. The distance of capture increases when the following parameters increase: the strength of the magnetic field, the diameter of MDCs, their magnetization and the number of MDCs / aggregate. A decrease in capture distance occurs when the blood velocity and the diameter of the blood vessels increase, and/or when their length decreases. A maximum capture distance of $x_{\max} \sim 12$ cm is obtained within diseased capillaries ($v_0 = 0.1$ mm/s, $L = 1.0$ mm, $\eta = 0.0028$ kg/ms, $\alpha = \pi/2$) when $H_0 = 500$ kA/m, $d = 3$ μm , $M_p = 1200$ kA/m, $\phi = 0.01$, $n = 3$. For normal capillaries ($v_0 = 10.0$ mm/s) with the same physiological and system parameters, the maximum distance of capture decreases to $x_{\max} \sim 8$ cm. This result suggests that differentiation in the retention of MDCs is possible even at the level of the capillaries if there is a physical separation between the normal and diseased blood vessels.

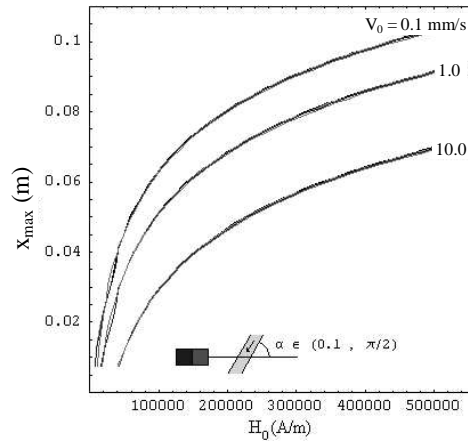


Fig. 11. The maximum capture distance (x_{\max}) of MDCs for arterioles and capillaries as a function of the magnetic field strength and for different orientations of the blood vessels. The blood vessels are pointing towards the magnetic source. The angle of inclination varies within the range $\alpha \in (0, \pi/2)$ and v_0 is a variable parameter. The remaining parameters are: $y_0 = 0.5$ mm, $\eta = 0.0028$ kg/ms, $d = 3.0$ μm , $M_p = 450$ kA/m, $a = 2.5$ cm, $v_0 = 0.1$ to 10.0 mm/s, $D = 12.0$ μm , $L = 1.0$ mm, and $\phi < 0.01$.

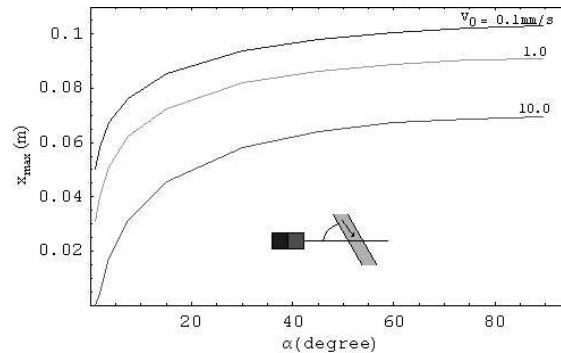


Fig. 12. The maximum capture distance (x_{\max}) of MDCs for arterioles and capillaries as a function of the orientation of the blood vessels. The blood vessels are pointing in the opposite direction to the magnetic source. The angle of inclination varies within the range $\alpha \in (0, \pi/2)$ and v_0 is variable parameter. The remaining parameters are: $y_0 = 0.5$ mm, $d = 3.0$ μ m, $M_p = 450$ kA/m, $a = 2.5$ cm, $v_0 = 0.1$ to 10.0 mm/s, $\eta = 0.0028$ kg/ms, $D = 12.0$ μ m, $L = 1.0$ mm, and $\phi < 0.01$.

Figs. 11 and 12 present the variation of x_{\max} for various orientations of the blood vessels with respect to the magnetic field source. There is no effect of blood vessel orientation when they point towards the magnetic field source (Figure 11). This phenomenon can be simply explained by the longer path of the MDCs along the magnetic force (Ox direction), which compensates the contribution to capture given by the drag force. However, when the blood vessels point in the opposite direction to the magnetic force, the situation is different, and x_{\max} decreases when the angle of inclination decreases. Therefore, in normal capillaries ($v_0 = 10.0$ mm/s), $x_{\max} \rightarrow 0$ when $\alpha \rightarrow 0^\circ$. In this limit situation the MDCs are mostly retained within diseased capillaries ($v_0 = 0.1$ mm/s, $x_{\max} \sim 5.0$ cm).

4. Conclusions

Computer simulations were developed to evaluate the focusing of MDCs of nano- and micrometer size within blood vessels situated at the surface and deep inside the human body. The results show that for an array of rectangular magnets, magnetic particles of diameter ≤ 3 μ m can be captured with high efficiency within the tumour capillaries and arterioles. The larger MPs (3 μ m) are preferentially retained at distances up to 12 cm in the capillary beds of the tumours, which have small luminal diameter and lower blood velocity than in normal blood vessels. However, within the small arteries these particles can be retained only at distance up to 3.5 cm. The presented results suggest the possibility of preferential MDCs targeting between normal tissues and those affected by tumours.

References

- [1] U. O. Hafeli, *Int. J. Pharm.* **277**, 19 (2004).
- [2] C. Alexiou, W. Arnold, R. J. Klein, F. G. Parak, P. Hulin, C. Bergemann, W. Erhardt, S. Wagenpfeil, A. S. Lubbe, *Cancer Res.* **60**, 6641 (2000).
- [3] A. S. Lubbe, C. Bergemann, H. Riess, F. Schriever, P. Reichardt, K. Possinger, M. Matthias, B. Dorken, F. Herrmann, R. Gurtler, P. Hohenberger, N. Haas, R. Sohr, B. Sander, A.-J. Lemnke, D. Ohlendorf, W. Huhnt and D. Huhn, *Cancer Res.* **56**, 4686 (1996).
- [4] A. S. Lubbe, C. Bergemann, J. Brock, D. G. McClure, J. Magn. Magn. Mater. **194**, 149 (1999).

- [5] O. Rotariu, N. J. C. Strachan, *J. Magn. Magn. Mater.* **293**, 639 (2005).
- [6] J. D. Jackson, *Classical Electrodynamics*, (Wiley, New York, 1975) p.185.
- [7] G. K. Batchelor, *An introduction in fluid dynamics*, (Cambridge University Press, London, 1970) p.233.
- [8] A. Satoh, R. W. Chantrell, S-I. Kamiyama, A. G. N. Coverdale, *J. Coll. Int. Sci.* **178**, 620 (1996).
- [9] O. Rotariu, N.J.C. Strachan, *Powder Tech.* **132**, 226 (2003).
- [10] N. Metropolis, A. W. Rosenbluth, M. N. Rosenbluth, A. H. Teller, E. Teller, *J. Chem. Phys.* **21**, 1087 (1953).
- [11] J. Liu, G. A. Flores, R. Sheng, *J. Magn. Magn. Mater.* **225**(1-2), 209 (2001).
- [12] J. H. P. Watson, *J. Appl. Phys.* **44**, 4209 (1973).